SERBIAN JOURNAL OF ELECTRICAL ENGINEERING
Vol. 7, No. 2, November 2010, 167-184

UDK: 621.313.333:681.586.7

Real Time Implementation of Adaptive Sliding Mode Observer Based Speed Sensorless Vector Control of Induction Motor

Karim Negadi[1], Abdellah Mansouri[2], Belkheir Khtemi[1]

Abstract: Sensorless induction motor drives are widely used in industry for their reliability and flexibility. However, rotor flux and speed sensors are required for vector control of induction motor. These sensors are sources of trouble, mainly in hostile environments, and their application reduces the drive robustness. The cost of the sensors is not also negligible. All the reasons lead to development of different sensorless methods for rotor flux and mechanical speed estimation in electrical drives. The paper deals with the speed estimators for applications in sensorless induction motor drive with vector control, which are based on application of model adaptive, based sliding mode observer methods. This paper presents the development and DSP implementation of the speed estimators for applications in sensorless drives with induction motor.

Keywords: Sensorless control, Induction motor drives, Sliding mode observer, MRAS, Modeling, Field oriented control, Dspace.

1 Introduction

Induction motor drives have been thoroughly studied in the past few decades and many vector control strategies have been proposed, ranging from low cost to high performance applications. In order to increase the reliability and reduce the cost of the drive, a great effort has been made to eliminate the shaft speed sensor in most high performance induction motor drive applications [1]. Speed estimation is an issue of particular interest with induction motor drives where the mechanical speed of the rotor is generally different from the speed of the revolving magnetic field. The advantages of speed sensorless induction motor drives are reduced hardware complexity and lower cost, reduced size of the drive motor, better immunity, elimination of the sensor cable, increased reliability and less maintenance requirements. The induction motor is however relatively difficult to control compared to other types of electrical motors. For high performance control, field oriented control is the

[1]Physics Engineering Laboratory, Ibn khaldoun University of Tiaret, Algeria, E-mail: negadi_k@yahoo.fr
[2]Laboratory of Automatics and Systems Analysis, Department of Electrical Engineering, E.N.S.E.T. Oran, Algeria, E-mail: ammansouri@yahoo.fr

most widely used control strategy [2]. This strategy requires information of the flux in motor; however the voltage and current model observers are normally used to obtain this information. Generally, using the induction motor state equations, the flux and speed can be calculated from the stator voltage and current values. This paper presents model adaptive based sliding mode observer for the proposed control.

2 Motor Model and Vector Control Strategy

The induction motor mathematical model in d-q coordinates established in a rotor flux oriented reference frame can be written as [3]:

$$v_{sd} = R_s i_{sd} + \frac{\mathrm{d}\Psi_{sd}}{\mathrm{d}t} - \omega_e \Psi_{sq} \tag{1}$$

$$v_{sq} = R_s i_{sq} + \frac{\mathrm{d}\Psi_{sq}}{\mathrm{d}t} + \omega_e \Psi_{sd} \tag{2}$$

$$0 = R_r i_{rd} + \frac{\mathrm{d}\Psi_{rd}}{\mathrm{d}t} - \omega_{sl} \Psi_{rq} \tag{3}$$

$$0 = R_r i_{rq} + \frac{\mathrm{d}\Psi_{rq}}{\mathrm{d}t} + \omega_{sl} \Psi_{rd} \tag{4}$$

where the stator and rotor flux linkages are given by:

$$\Psi_{sd} = L_s i_{sd} + L_m i_{rd} \tag{5}$$

$$\Psi_{sq} = L_s i_{sq} + L_m i_{rq} \tag{6}$$

$$\Psi_{rd} = L_r i_{rd} + L_m i_{sd} \tag{7}$$

$$\Psi_{rq} = L_r i_{rq} + L_m i_{sq} \tag{8}$$

The state space representation of the induction motor with the stator currents and the rotor flux linkages components as state variables can be written as [4]:

$$\begin{bmatrix} \frac{\mathrm{d}}{\mathrm{d}t} i_{sd} \\ \frac{\mathrm{d}}{\mathrm{d}t} i_{sq} \\ \frac{\mathrm{d}}{\mathrm{d}t} \Psi_{rd} \\ \frac{\mathrm{d}}{\mathrm{d}t} \Psi_{rq} \end{bmatrix} = \boldsymbol{A} \begin{bmatrix} i_{sd} \\ i_{sq} \\ \Psi_{rd} \\ \Psi_{rq} \end{bmatrix} + \begin{bmatrix} \frac{1}{\sigma L_s} & 0 \\ 0 & \frac{1}{\sigma L_s} \\ 0 & 0 \\ 0 & 0 \end{bmatrix} \begin{bmatrix} v_{sd} \\ v_{sq} \end{bmatrix}, \tag{9}$$

where

$$\boldsymbol{A}=\begin{bmatrix} -\left(\frac{R_s}{\sigma L_s}+\frac{1-\sigma}{\sigma T_r}\right) & \omega_e & \frac{L_m}{\sigma L_s L_r T_r} & \left(\frac{L_m}{\sigma L_s L_r}\right).\omega_r \\ -\omega_e & -\left(\frac{R_s}{\sigma L_s}+\frac{1-\sigma}{\sigma T_r}\right) & -\left(\frac{L_m}{\sigma L_s L_r}\right).\omega_r & \frac{L_m}{\sigma L_s L_r T_r} \\ \frac{L_m}{T_r} & 0 & \frac{-1}{T_r} & (\omega_e-\omega_r) \\ 0 & \frac{L_m}{T_r} & -(\omega_e-\omega_r) & \frac{-1}{T_r} \end{bmatrix},$$

T_r is the rotor time constant and is given by $T_r = L_r/R_r$ and σ is the leakage coefficient given by $\sigma = 1-\frac{L_m^2}{L_r L_s}$.

The electromagnetic torque and the rotor speed are given by:

$$T_{em} = \frac{3}{2} p \frac{L_m}{L_r}(\Psi_{rd} i_{sq} - \Psi_{rq} i_{sd}), \tag{10}$$

where:

R_s and R_r are the stator and rotor winding resistances;

L_s, L_m and L_r are the stator, mutual and rotor inductances;

p is the number of pole pairs;

ω_e, ω_r and ω_{sl} are the synchronous, rotor and slip speed in electrical rad/s;

v_{sd}, v_{sq}, i_{sd}, i_{sq}, Ψ_{rd} and Ψ_{rq} are stator voltage, stator current and rotor flux *d-q* components in the rotor flux oriented reference frame;

T_{em} and T_l are the electromagnetic torque and the load torque respectively;

J and f are the motor inertia and viscous friction coefficient respectively.

Under the rotor flux orientation conditions the rotor flux is aligned on the d-axis of the d-q rotor flux oriented frame and the rotor flux equations can be written as:

$$\Psi_{rq} = 0 \tag{11}$$

$$\Psi_{rd} = L_m i_{sd} \tag{12}$$

The electromagnetic torque equation can be written as:

$$T_{em} = \frac{3}{2} p \frac{L_m}{L_r} \Psi_r i_{sq} = K_t i_{sq}, \tag{13}$$

where K_t is the torque constant given by:

$$K_t = \frac{3}{2} p \frac{L_m}{L_r} \Psi_r . \tag{14}$$

3 Model Reference Adaptive Systems (MRAS)

The basic concept of MRAS is the presence of a reference model which determines the desired states and an adaptive (adjustable) model which generates the estimated values of the states. The error between these states is fed to an adaptation mechanism to generate an estimated value of the rotor speed which is used to adjust the adaptive model. This process continues till the error between two outputs tends to zero [4, 5]. Basic equations of rotor flux based-MRAS can be written as:

$$\Psi_r = \left(\frac{L_r}{L_m} \right) \left[\int (v_s - R_s i_s) \, \mathrm{d}t - L_s i_s \right], \tag{15}$$

$$\hat{\Psi}_r = \left(\frac{1}{T_r} \right) \int (L_m i_s - \hat{\Psi}_r - \hat{\omega} T_r \hat{\Psi}_r) \, \mathrm{d}t . \tag{16}$$

The reference model (15) is based on stator equations and is therefore independent of the motor speed, while the adaptive model (16) is speed-dependant since it is derived from the rotor equation in the stationary reference frame. To obtain a stable nonlinear feedback system, a speed tuning signal (ε_ω) and a PI controller [6] are used in the adaptation mechanism to generate the estimated speed. The speed tuning signal and the estimated speed expressions can be written as:

$$\varepsilon_\omega = \Psi_{rq} \hat{\Psi}_{rd} - \Psi_{rd} \hat{\Psi}_{rq}, \tag{17}$$

$$\hat{\omega} = \left\{ K_p + \frac{K_i}{s} \right\} \varepsilon_\omega, \tag{18}$$

where K_p and K_i are the proportional and integral constants, respectively.

Generally the MRAS observer gives satisfactory speed estimation in the high and medium speed regions. When working at low speed the observer performance deteriorates due to integrator drift and initial condition problems and sensitivity to current measurement noise. Therefore a sliding mode observer is proposed to replace the conventional adaptive model (16) (Fig. 1) to improve

the MRAS scheme performance at load condition, reversal speed and low speed region [7].

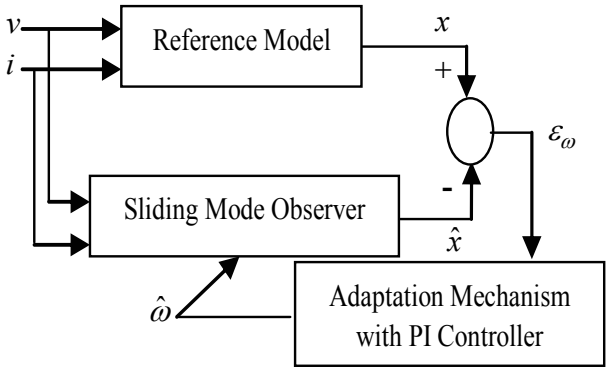

Fig. 1 – MRAS *with sliding mode observer.*

4 The Propose Sliding Mode Observer

Considering only the four first equations of the induction motor model and noting $\hat{x}_1, \hat{x}_2, \hat{x}_3, \hat{x}_4$ the observation of x_1, x_2, x_3, x_4 respectively. The observer model is a copy of the original system, where added correctors are gains with switching terms [8]. Let, $\Lambda_1, \Lambda_2, \Lambda_3$ and Λ_4, are the observer gains with $\Lambda_j = \begin{bmatrix} \Lambda_{j1} & \Lambda_{j2} \end{bmatrix}$ for $j \in \{1,2,3,4\}$

$$i_s = \begin{bmatrix} \mathrm{Sign}(S_1) \\ \mathrm{Sign}(S_2) \end{bmatrix}, \tag{19}$$

with:

$$S = \begin{bmatrix} S_1 \\ S_2 \end{bmatrix} = \Gamma \begin{bmatrix} x_1 - \hat{x}_1 \\ x_2 - \hat{x}_2 \end{bmatrix}, \quad \Gamma = \frac{1}{\beta} \begin{bmatrix} \frac{K}{T_r} & -p\omega K \\ p\omega K & \frac{K}{T_r} \end{bmatrix}, \quad \beta = \left[\frac{K}{T_r}\right]^2 + p^2\omega^2 K^2 .$$

The choice of Γ is made to get a simple observer gain synthesis. Setting $e_j = x_j - \hat{x}_j$ for $j \in \{1,2,3,4\}$, the estimation error dynamics is given by

$$\dot{e}_1 = \frac{K}{T_r} e_3 + p\omega K e_4 - \Lambda_1 i_s \tag{20}$$

$$\dot{e}_2 = \frac{K}{T_r} e_4 - p\omega K e_3 - \Lambda_2 i_s \tag{21}$$

$$\dot{e}_3 = \frac{1}{T_r} e_3 - p\omega e_4 - \Lambda_3 i_s \tag{22}$$

$$\dot{e}_4 = \frac{1}{T_r} e_4 + p\omega e_3 - \Lambda_4 i_s \tag{23}$$

One has the following result.

Assume that the state variables x_3 and x_4 are bounded, and consider system (20) at (24) with the following observer gain matrices [9]:

$$\begin{bmatrix} \Lambda_{11} & \Lambda_{21} \\ \Lambda_{12} & \Lambda_{22} \end{bmatrix} = \Gamma^{-1} \begin{bmatrix} \delta_1 & 0 \\ 0 & \delta_2 \end{bmatrix},$$

$$\begin{pmatrix} \Lambda_{31} & \Lambda_{32} \\ \Lambda_{41} & \Lambda_{42} \end{pmatrix} = \begin{pmatrix} \dfrac{\left(q_1 - \dfrac{1}{T_r}\right)}{\delta_1} & \dfrac{-P\omega}{\delta_2} \\ \dfrac{p\omega}{\delta_1} & \dfrac{\left(q_2 - \dfrac{1}{T_r}\right)}{\delta_2} \end{pmatrix}$$

where

$$\delta_1 = \rho_3 + |\hat{x}_3| + a_{\max} |e_1| + b_{\max} |e_2|$$

$$\delta_2 = \rho_4 + |\hat{x}_4| + b_{\max} |e_1| + a_{\max} |e_2|$$

$$a_{\max} = 2T_r p^2 K \eta_1 \eta_2 \,,\; b_{\max} = pT_r^2 \eta_2 \left(\frac{1}{K} + 2p^2 \eta_1^2 \right),$$

and η_1, η_2 are two known positive parameters.

Since

$$|x_3| \le \rho_3 \,,\; |x_4| \le \rho_4 \text{ and } q_1, q_2 > 0 \,.$$

then $\begin{bmatrix} e_1 & e_2 & e_3 & e_4 \end{bmatrix}^T$ converge to zero.

It should be noted that our observer is robust in face of modeling uncertainty and error in the measurements [10].

The implementation of the nonlinear sliding mode observer is easy using the Embedded MATLAB function block is based on an M-file written in the MATLAB language because it can be supported by RTI (Real Time Interface). The convergence of the algorithm is assured with simple time $T_e = 1.5 \cdot 10^{-4}$ s, use Euler method.

5 Description of Laboratory Setup

The adaptive sliding mode speed observer has been tested experimentally on a suitable test setup (Fig. 2). The test setup consists of the following:

- Three-phase induction motor with rated values shown in appendix;
- Synchronous machine for loading the induction motor;
- Electronic power converter: three-phase diode rectifier and VSI composed of three IGBT modules without any control system;
- Electronic card with voltage sensors (model LEM LV 25-P) and current sensors (model LEM LA 55-P) for monitoring the instantaneous values of the stator phase voltages and currents;
- Voltage sensor (model LEM CV3-1000) for monitoring the instantaneous value of the dc-link voltage;
- Incremental encoder (model RS 256-499, 2500 pulses per round), only for comparison measurements;
- dSPACE card (model DS1104) with a PowerPC 604e at 400 MHz and a fixed-point digital signal processor (DSP) TMS320F240.

Fig. 2 – *Experimental setup.*

During the real-time operation of the control algorithm, the supervision and capturing of the signals can be done by the Control Desk software provided with the DSP board.

6 Experimental Results and Discussion

The application of proposed reconstruction technique and estimation of feedback signals is illustrated by a computer simulation. Flux reference is set to its rated value and the dc link voltage is 500 V. Some experimental results were provided to demonstrate the effectiveness of the proposed observer technique.

Scenario 1: First experiment, the target speed is changed from 0 rpm to 1490 rpm at 1.5 s at no load applied. Fig. 3 shows the experimental result of a speed at free acceleration using the estimation of speed. Additionally, the real speed is measured and compared. It can be seen that there is a very good accordance between real and estimated speed without any steady state error.

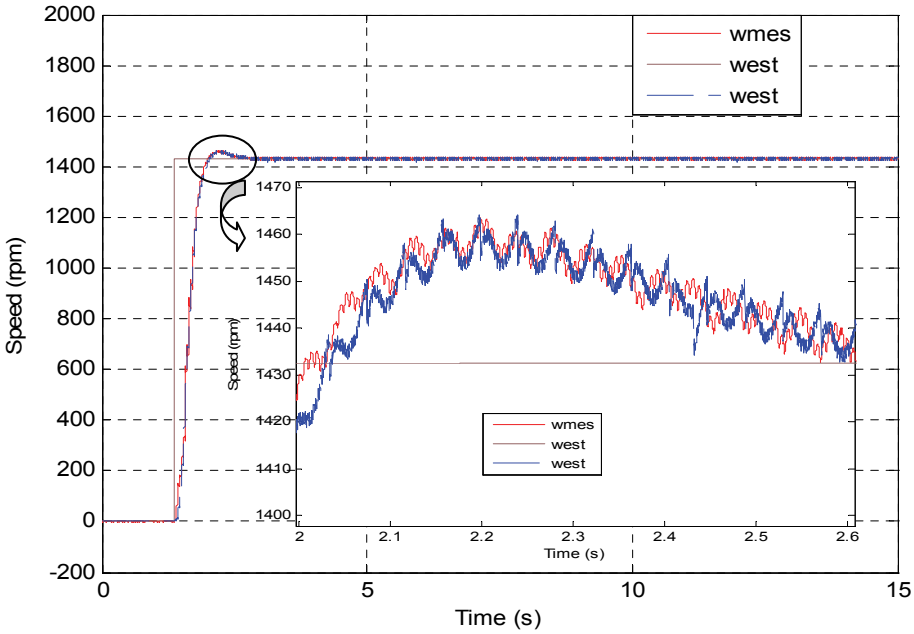

Fig. 3 – *The reference, actual and estimated speed at no load condition.*

Fig. 4 depicts the trajectories of the electromagnetic torque (a), estimated and measured stator currents evolution (b). It should be noted that the amplitude of the torque ripple is slightly higher.

Scenario 2: Fig. 5 shows the speed sensorless control performance where the load was applied and omitted. The estimated speed coincides exactly with the real speed even the load torque application instant. From these results, it is shown that the proposed speed-sensorless control algorithm has good performances.

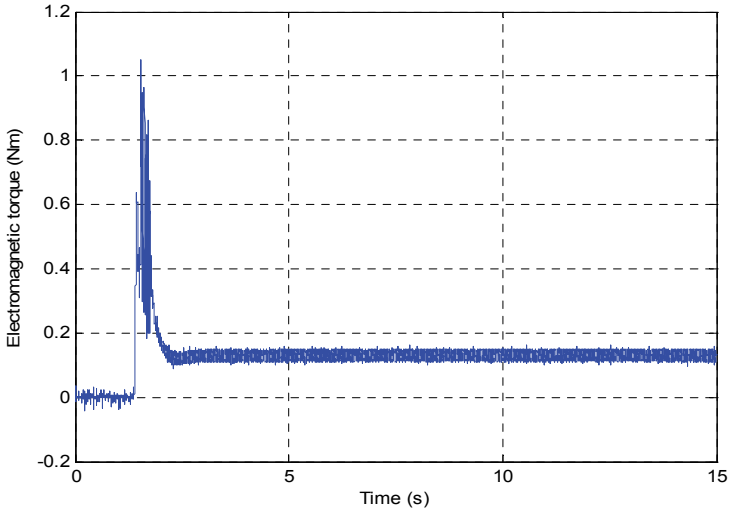

a)

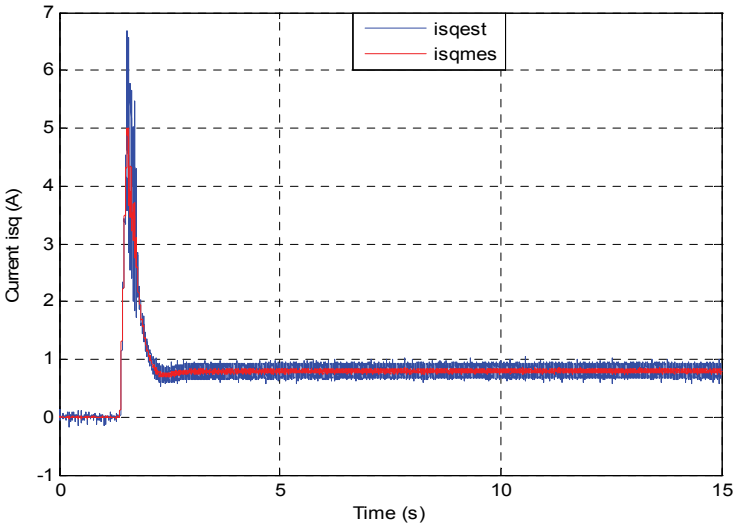

b)

Fig. 4 – a) *Response electromagnetic torque*; b) *Estimated stator currents evolution*.

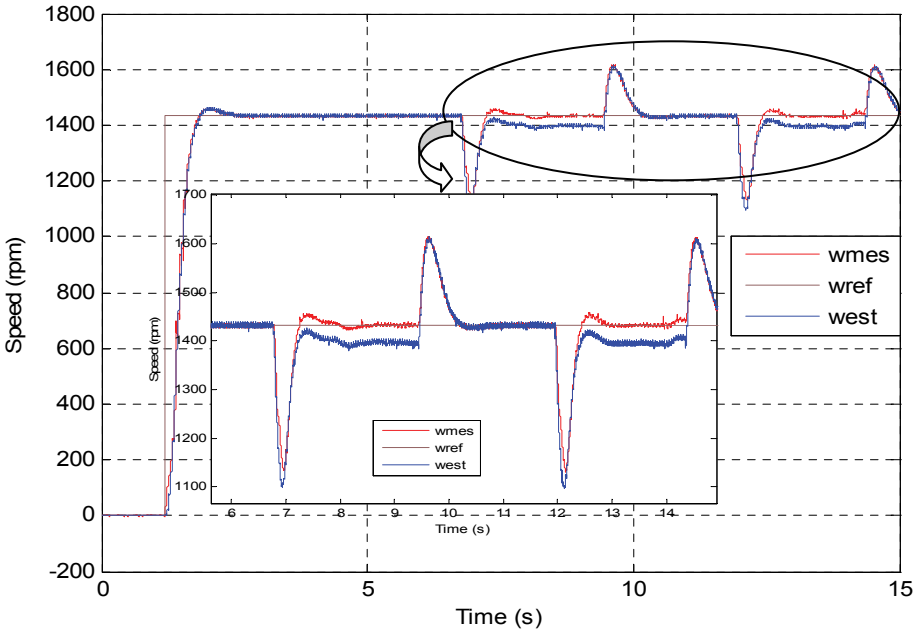

Fig. 5 – *The reference, actual and estimated speed at speed applied a load at* 5-7-13-15 s.

The real and estimated stator currents and the estimated electromagnetic torque, when the motor is running at high speed with load applied, are given by Figs. 6a and 6b. these figures show that the real and the estimated stator currents, the estimates electromagnetic torque are in close agreement.

Scenario 3: The reference speed is set to 1400 rpm at $t = 2\,\text{s}$. Then the set point is changed to -1400 rpm at $t = 10\,\text{s}$ without any load (Fig. 7). It is clear that the speed response exhibits good performances at both dynamics regimes. The result clearly shows that the estimated speed follows the actual speed and the error is not significant.

The results shown in Figs. 8a and 8b illustrate, the electromagnetic torque, actual and estimated stator currents trajectory. These results made the drive remain stable and this condition can be maintained indefinitely.

Scenario 4: The controller was tested under with the speed dependent load produced by the synchronous machine. The reversal speed response of the motor is shown in Fig. 6 at high speeds without load and in Fig. 7 under different levels of load torque.

From inspection of Figs. 8a and 8b, it is possible to verify the excellent behavior of the proposed algorithm. In fact, the error on the estimation both of

the stator currents and of the electromagnetic torque are always very small (<2%, by referring to the actual values). Fig. 7 shows too the error between real and estimated speeds. Figs. 4 and 5 indicate that the estimated value also tracks its true value very closely in both the forward and reverse directions.

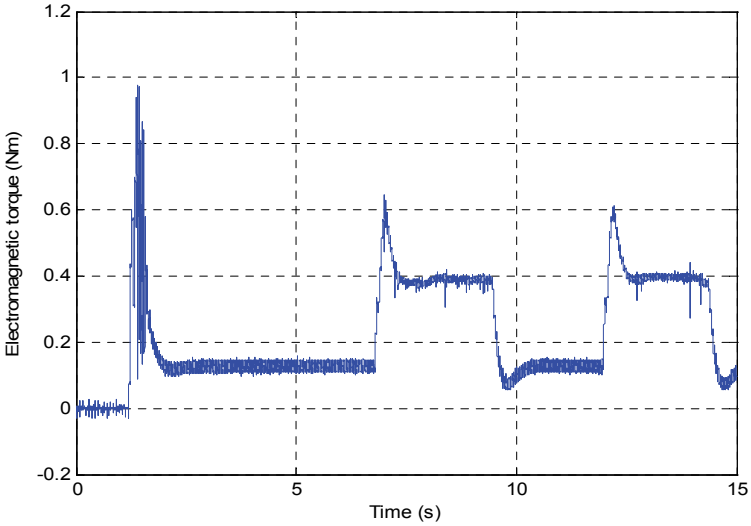

a)

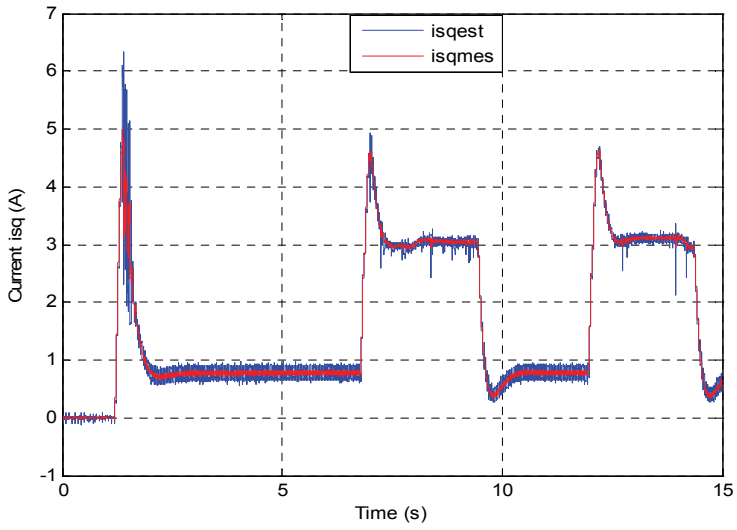

b)

Fig. 6 – a) *Response electromagnetic torque*; b) *Estimated stator currents evolution*.

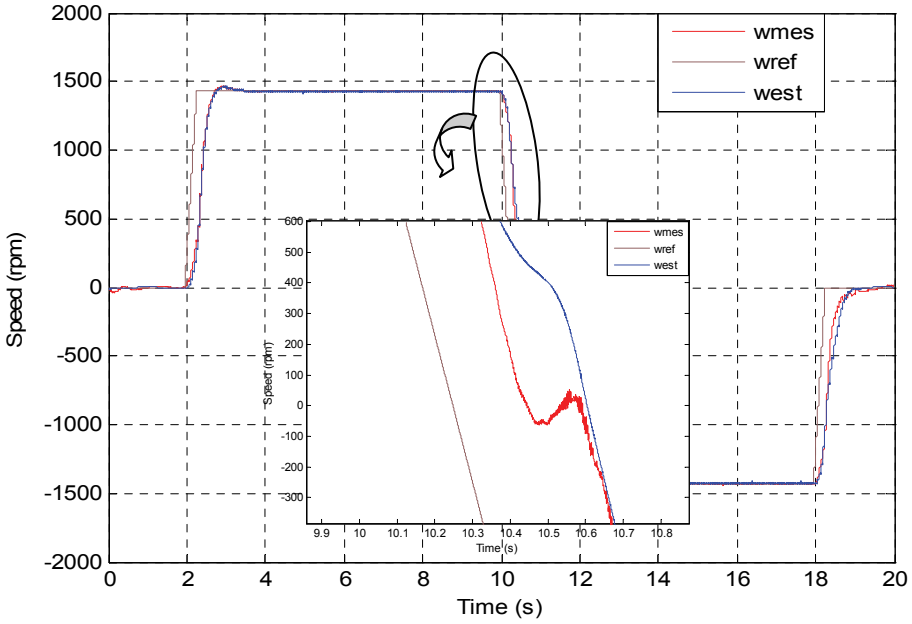

Fig. 7 – *The reference, actual and estimated speed at speed reversal with no load condition.*

Scenario 5: To test the performance of the control drive at low speed without load. We applied a changing of the speed reference from 100 rpm to -100 rpm at $t = 10\,\mathrm{s}$. Speed control performance is shown in Fig. 11.

We can see that the speed follow perfectly the speed reference. However, it is important to note that the control system demonstrates a good performance even under those variations. We note that the performance degrades as approaching the low speed region and fails to provide large oscillations. Figs. 12a and 12b show torque and stator current estimation in the low speed operation.

Excellent tracking performance was obtained no study state error and no overshoot and control performance of the drive is acceptable for load disturbance. The gotten results show the effectiveness of the proposed control scheme.

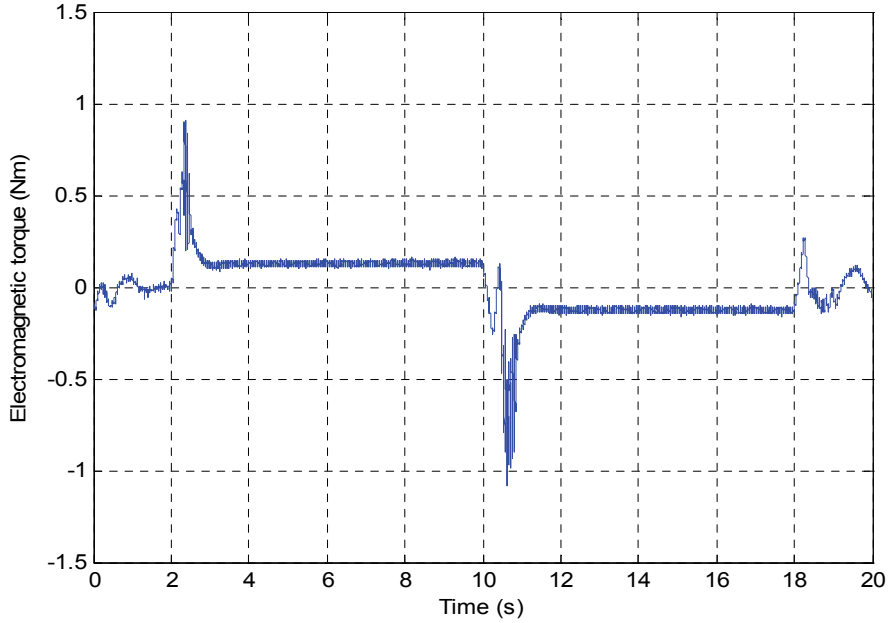

a)

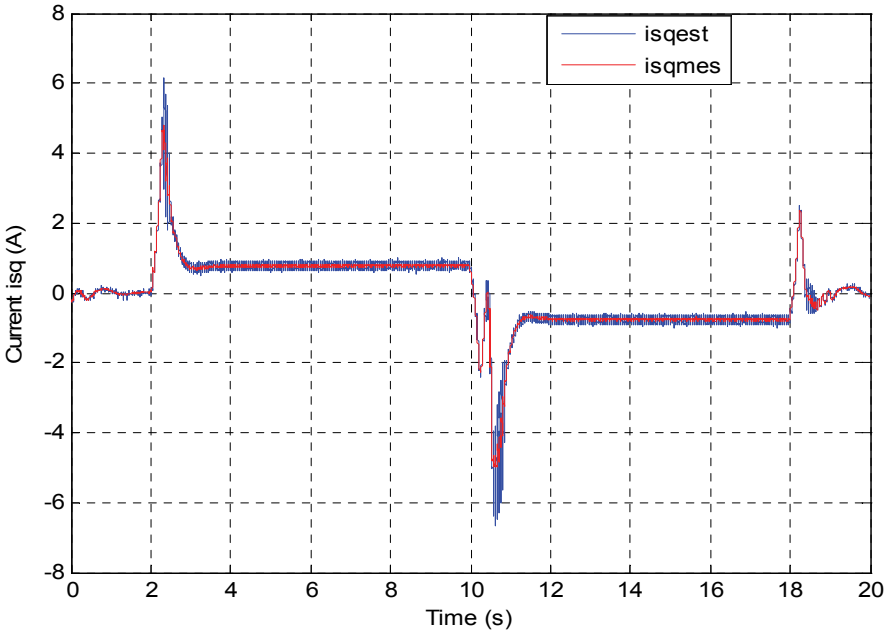

b)

Fig. 8 – a) *Response electromagnetic torque*, b) *Estimated stator currents evolution*.

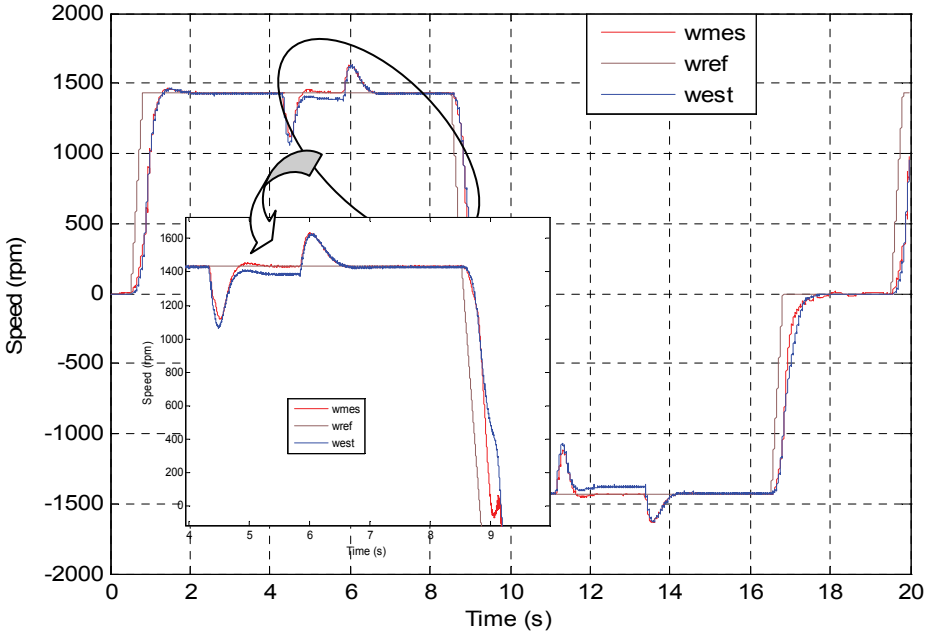

Fig. 9 – *The reference, actual and estimated speed at reversal speed with a load applied at* 5-7-13-15 s.

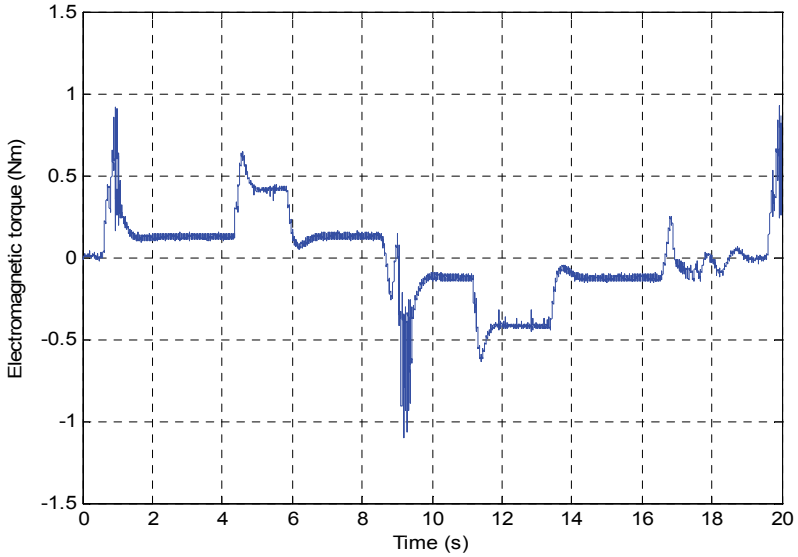

Fig. 10a – *Response electromagnetic torque.*

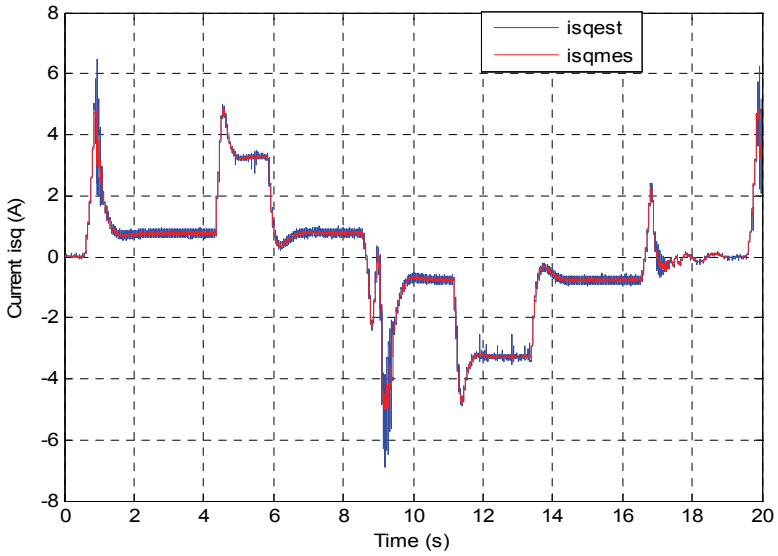

Fig. 10b – *Estimated stator currents evolution.*

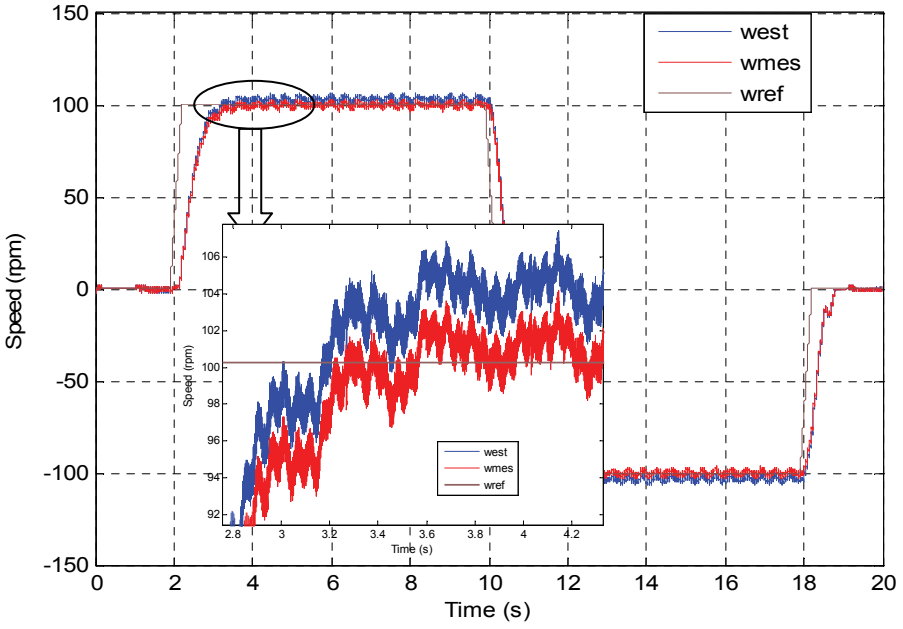

Fig. 11 – *The reference, actual and estimated speed at speed applied at low speed with reversal speed.*

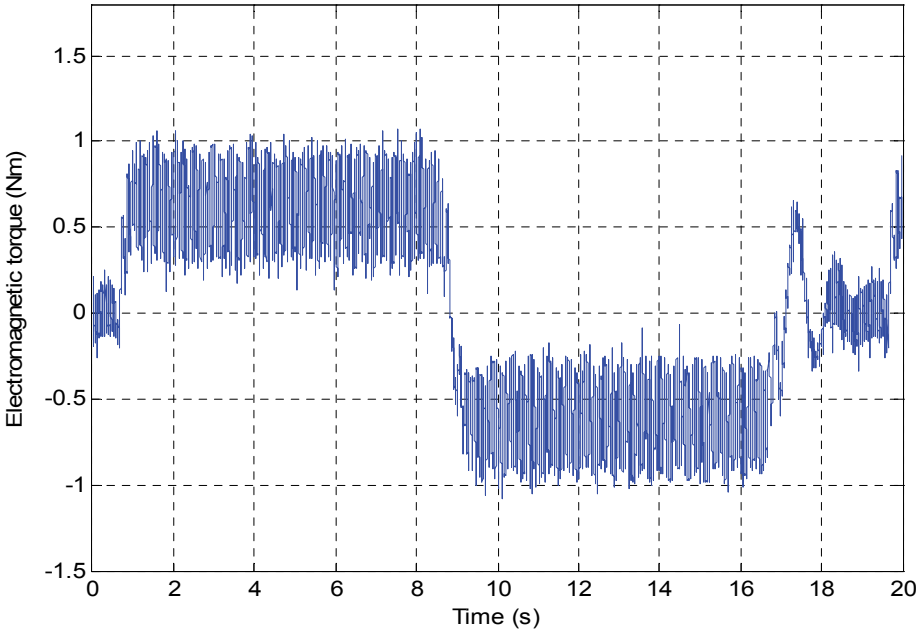

a)

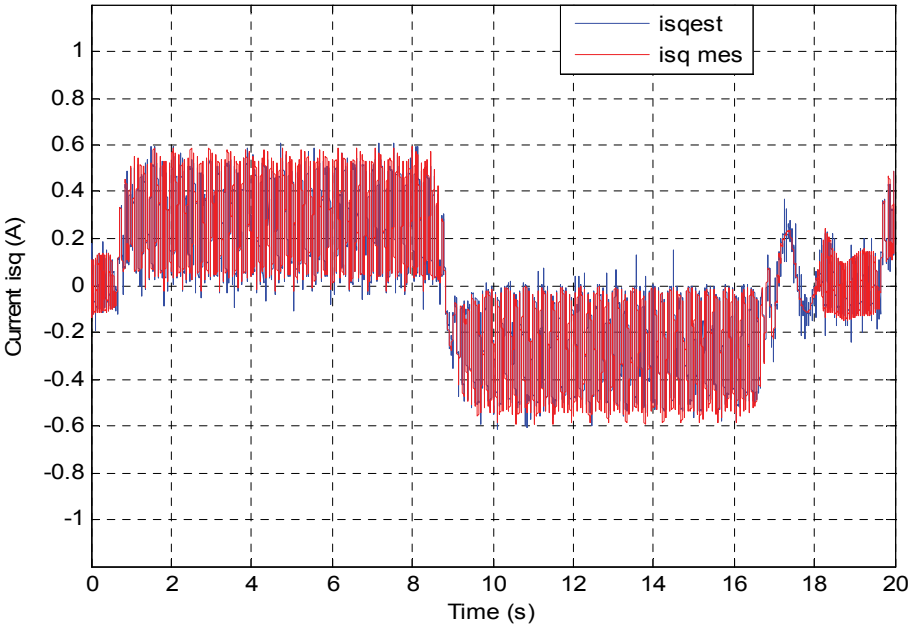

b)

Fig. 12 – a) *Response electromagnetic torque*; b) *Estimated stator currents evolution*.

7 Conclusion

Both observers presented in the paper can estimate the speed in an electrical drive system. The values of the speed estimated on-line can be used by the control of the electrical drive systems in speed range. For both observers the drive system must be endowed an acquisition system for the electrical variables, which helps to calculate the electromagnetic torque of the electrical motor, who is based on the generally equation of motion the same in every drive system for any kind of electrical motor. The estimation performances of both observers are comparable. For the observers presented in this paper the drive's parameters were considered constant.

The main features are the following:

- The instantaneous speed is estimated by Adaptive sliding mode observer.
- To obtain a high-dynamic current sensorless control, a current to voltage feed forward decoupling and a dynamic correction are applied.
- Moreover, an accurate dynamic limitation of the real electromagnetic torque is obtained.
- Extensive experimental results using an induction motor drive prove high-dynamic performances and robustness of the proposed control structure in dSPACE environment.

8 Appendix

R_s = 11.8Ω, R_r = 11.3085Ω, L_s = L_r=0.5568 H, L_m = 0.6585 H,
J = 0.0020 kg·m^2, f = 3.1165e–004 Nm/rad/s, p=1.

9 References

[1] R. Magurean , C. Ilas, V. Bostan, M. Cuibus, V. Radut: Luenberger, Kalman, Neural Observers and Fuzzy Controllers for Speed Induction Motor, Buletinul Institutului Politehnic Iasi Tomul XLVI (L), FASC 5, 2000.

[2] A. Bentaallah, A. Meroufel, A. Bendaoud, A. Massoum, M.K. Fellah: Exact Linearization of an Induction Machine with Rotoric Flux Orientation, Serbian Journal of Electrical Engineering Vol. 5, No. 2, Nov. 2008, 217 – 227.

[3] M. Marcu, I. Utu, L. Pana, M. Orban: Computer Simulation of Real Time Identification for Induction Motor Drives, International Conference on Theory and Applications of Mathematics and Informatics - ICTAMI 2004, Thessaloniki, Greece, pp. 295 – 305.

[4] A. Chikhi, M. Djarallah, K. Chikhi: A Comparative Study of Field-oriented Control and Direct-torque Control of Induction Motors using an Adaptive Flux Observer, Serbian Journal of Electrical Engineering Vol. 7, No. 1, May 2010, 41 – 55.

[5] R.B. Gimenez: High Performance Sensorless Vector Control of Induction Motor Drives, PhD Thesis, University of Nottingham, Dec. 1995.

[6] C. Schauder: Adaptive Speed Identification for Vector Control of Induction Motor without Rotational Transducers, IEEE Transactions on Industry Applications, Vol. 28, No. 5, Sept/Oct. 1992, pp. 1054 – 1061.

[7] M. Messaoudi, L. Sbita, M.B. Hamed, H. Kraiem: MRAS and Luenberger Observer based Sensorless Indirect Vector Control of Induction Motors, Asian Journal of Information Technology, Vol. 7, No. 5, 2008, pp. 232 – 239.

[8] M. Djemai, J. Hernandez, J.P Barbot: Nonlinear Control with Flux Observer for Singularly Perturbed Induction Motor, IEEE Conference on Decision and Control, Vol. 4, San Antonio, TX, USA, Dec. 1993, pp. 3391 – 3396.

[9] S. Drakunov, S. Utlun: Sliding Mode Observers, 34th IEEE CDC, New Orleans, LA, USA, 1995, pp. 3376 – 3378.

[10] A.S. Iong, L. Gelman: Advances in Electrical Engineering and Computational Science, Lecture Notes in Electrical Engineering, Vol. 39, Springer, 2009.